

702 APPENDIX

703

704 A ANONYMIZED CODE

705

706 For an anonymized version of our code, please see: anonymous.4open.science/r/polysona

707

708 B WEIGHT-MIXING IMPLEMENTATION

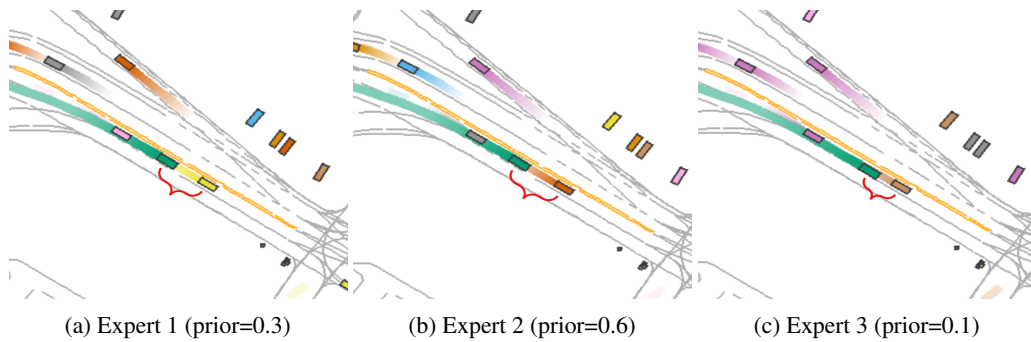
709

710 **PyTorch-Style Forward Pass of Weight-Mixing Mixture-of-LoRA Layer**

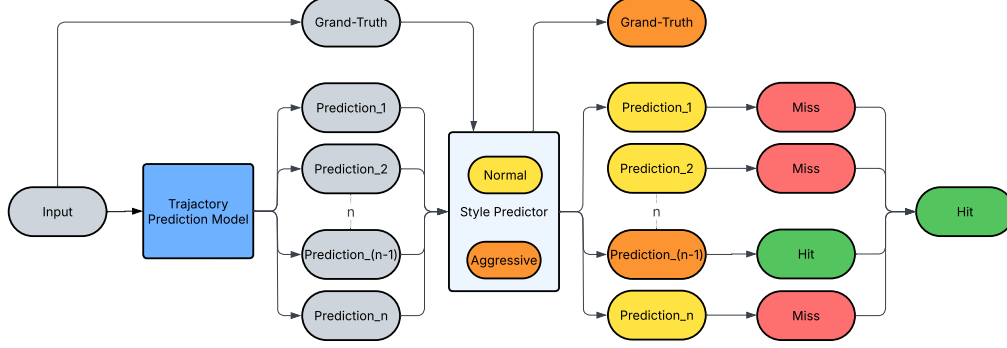
```

711
712     expert_alphas = router(...) # (b, num_experts)
713
714     expert_weight_A = (expert_alphas[..., None, None] * self.
715         expert_weight_A[None]).sum(
716             dim=1
717         ) # (b, r, in_features)
718     expert_weight_B = (expert_alphas[..., None, None] * self.
719         expert_weight_B[None]).sum(
720             dim=1
721         ) # (b, out_features, r)
722
723     output = torch.einsum(
724         "bi,bri->br", x, expert_weight_A
725     ) # (b, in_features) @ (b, r, in_features) -> (b, r)
726     output = torch.einsum(
727         "br,bor->bo", output, expert_weight_B
728     ) # (b, r) @ (b, out_features, r) -> (b, out_features)
729     output = self.dropout(output) # (b, out_features)
730
731     output = F.linear(x, w0, b0) + output # w0x + BAx + b0
732
733
734
735
736
737
738
739
740
741
742
743
744
745
746
747
748
749
750
751
752
753
754
755

```

756 C QUALITATIVE RESULTS ON ARGOVERSE
757

759
760
761
762
763
764
765
766
767
768
769
770 **Figure 5: Qualitative result: Rollouts on a lane change scenario with different experts on**
771 **Ours+CAT.** We show how different experts behave under the same lane change scenario, where
772 the goal is to lane change between two agents. While rollouts from Expert 1 and 2 are very similar
773 (maintaining at least one vehicle length from the leading vehicle), Expert 3, which has the lowest
774 prior probability, predicts a trajectory with much smaller headway distance. Animations of these
775 scenarios are better visualized on our project website, linked in the abstract.

776 D STYLE CONSISTENCY METRIC VISUALIZATION
777

779
780
781
782
783
784
785
786
787
788
789
790 **Figure 6: Style Consistency Metric.** Given a driving scenario (“Input”), the black-box trajectory
791 predictor generates n candidate futures ($\text{Prediction}_1, \dots, \text{Prediction}_n$). A learned style predictor
792 then assigns each candidate—and the true future (“Ground-Truth”)—to one of two clusters (e.g.
793 “Normal” vs. “Aggressive”). If at least one of the n predicted trajectories shares the same style
794 label as the ground-truth, the sample is marked a *Hit*; otherwise it is a *Miss*. This hit/miss outcome
795 directly measures whether the model’s multi-modal outputs *cover* the driver’s actual style, beyond
796 conventional displacement errors.

797 E STYLE CONSISTENCY METRIC
798

801 To explicitly measure a model’s ability to cover the correct driving style, as shown in Figure 6, we
802 propose the *Style Miss Rate* a style consistency metric based on kinematic clustering following the
803 clustering methodology introduced in (Zheng et al., 2025), and a hit/miss criterion:

804 **Extract kinematic statics:** For each trajectory τ , compute a feature vector

$$\phi(\tau) = [\max_t |a(t)|, \text{Var}(a), \text{Var}(v), \gamma]^T \in \mathbb{R}^d, \quad (8)$$

805 where a is acceleration (with $\max_t |a(t)|$ denoting the peak absolute acceleration over the trajectory,
806 i.e. the highest instantaneous acceleration magnitude), v is speed, and

810

$$\gamma = \frac{\text{Var}(j(t))}{\mathbb{E}[j(t)]}$$

813 is the jerk-variance ratio as defined in Murphrey et al. (2009).

814 **Learn style clusters:** Fit a Gaussian Mixture Model (GMM) with $k = 2$ on the set of all ground-truth
815 kinematic embeddings in the evaluation set $\{\phi(\tau_n^*)\}_{n=1}^N$, yielding a cluster assignment function

817

$$818 \quad C(\phi) \in \{"\text{normal}", "\text{aggressive}"\}. \quad (9)$$

819

820 Normal and aggressive are assigned based on the mean speed of each cluster. A cluster with higher
821 mean speed will be assigned as aggressive.

822 **Assign styles to predictions:** For each sample n , let $\{\hat{\tau}_{n,i}\}_{i=1}^6$ be the six predicted trajectories.
823 Define

$$824 \quad s_n^* = C(\phi(\tau_n^*)), \quad s_{n,i} = C(\phi(\hat{\tau}_{n,i})). \quad (10)$$

825

826 **Define hit/miss:** A *hit* occurs if at least one predicted style matches the ground-truth style:

$$827 \quad \text{Hit}_n = \{\exists i : s_{n,i} = s_n^*\}, \quad \text{Miss}_n = 1 - \text{Hit}_n. \quad (11)$$

828

829 **Style Miss Rate:** The overall metric is

$$830 \quad \text{SMR} = \frac{1}{N} \sum_{n=1}^N \text{Miss}_n. \quad (12)$$

831

832 By construction, the SMR goes beyond pure spatial accuracy: it measures whether the model
833 “covers” the driver’s true style among its multi-modal outputs. A style-agnostic predictor may achieve
834 low ADE/FDE by clustering its modes around average behavior, but will incur a high miss rate
835 on aggressive samples. In contrast, a style-aware model—conditioned on inferred driving-style
836 embeddings—should include at least one candidate trajectory whose kinematics align with the true
837 style, yielding a lower SMR.

838

839

840

841

842

843

844

845

846

847

848

849

850

851

852

853

854

855

856

857

858

859

860

861

862

863

864 F STYLE MISS RATE EVALUATION ON ABLATION VARIANTS
865

866 To further assess how each component of our mixture-of-experts framework contributes to style
867 coverage, we compute the Style Miss Rate (SMR) on the same ablation variants presented in Table 4.
868 That is, for each model variant—removing reconstruction, KL loss, entropy regularization, etc.—we
869 evaluate how often none of its multi-modal predictions match the true driving style cluster. The
870 resulting SMR values are reported in Table 6. This analysis shows that the ablations which most
871 degrade traditional error metrics (e.g. reconstruction and KL removal) also incur the largest increases
872 in SMR, indicating a direct link between component contributions and the model’s ability to cover
873 the driver’s style.

874
875 Table 6: **Style Miss Rate (SMR) for each ablation variant.**

Ours	SMR \downarrow
+LinearRouter	0.2246
+Full Finetuning	0.2033
-Social Forces	0.2229
-Context Features	0.2236
-KL Loss	0.2267
-Reconstruction	0.2263
-Expert Entropy Loss	0.2260

918 **G HOW DOES THE MODEL REASON? TAKING A LOOK AT THE SALIENCY
919 MAPS.**

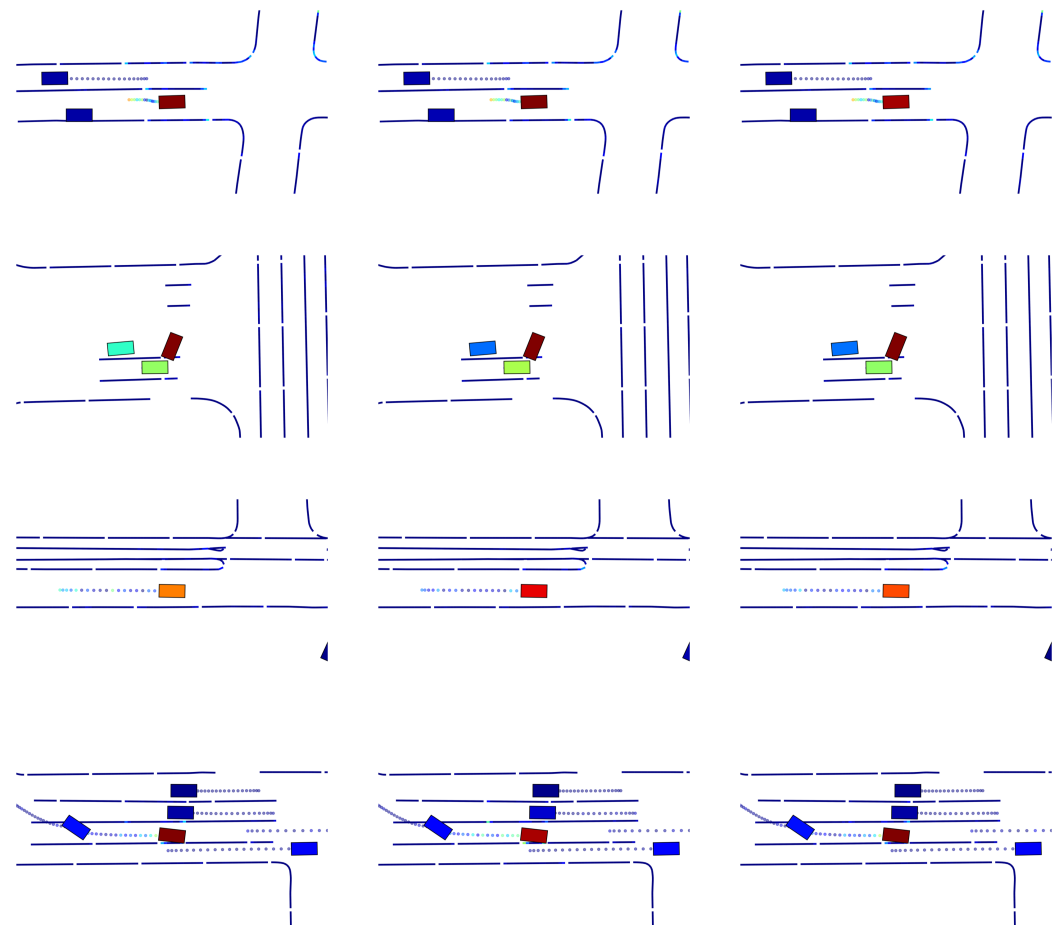
921 To gain insight into which input features the model attends when forecasting agent trajectories, we
922 compute saliency maps by measuring the sensitivity of the most likely predicted trajectory with
923 respect to each input feature. Formally, let $X = \{A_{in}, M_{in}\}$ denote the concatenation of historical
924 object trajectories A_{in} and map polylines M_{in} . If \hat{p}_τ is the probability of trajectory τ , then let
925 $\hat{\tau}^* = \arg \max_\tau \hat{p}_\tau$ be the most likely predicted trajectory after a forward pass from a model. Then,
926 we compute the gradient

$$\nabla_X \hat{\tau}^* = \frac{\partial \hat{\tau}^*}{\partial X}$$

927 via back-propagation, and form the saliency map
928

$$S(X) = \log(\|\nabla_X \hat{\tau}^*\|_2 + 1).$$

929 We use logarithmic scaling above to better display nuances in smaller gradient magnitudes. For
930 visualizing this saliency map, we render the map polylines and the agents' historical trajectories
931 colored using $S(X)$ on the "jet" color scheme (dark blue to green to dark red). Warmer colors
932 highlight map segments or agent trajectories that the model deems more important for predicting
933 future trajectories. Likewise, lighter colors highlight areas of less importance. Each agent vehicle
934 is also colored on the same scale based on the maximum saliency value of its historical trajectory. We
935 generate this visualization for MTR+Actions, Ours+CAT, and Ours+MoV:
936



970 **Figure 7: Visualization of scenario feature saliency (Continued on the next page).** Saliency
971 maps are visualized for 10 randomly selected scenarios from Argoverse on MTR+Actions (Left),
972 Ours+CAT (Middle), and Ours+MoV (Right).

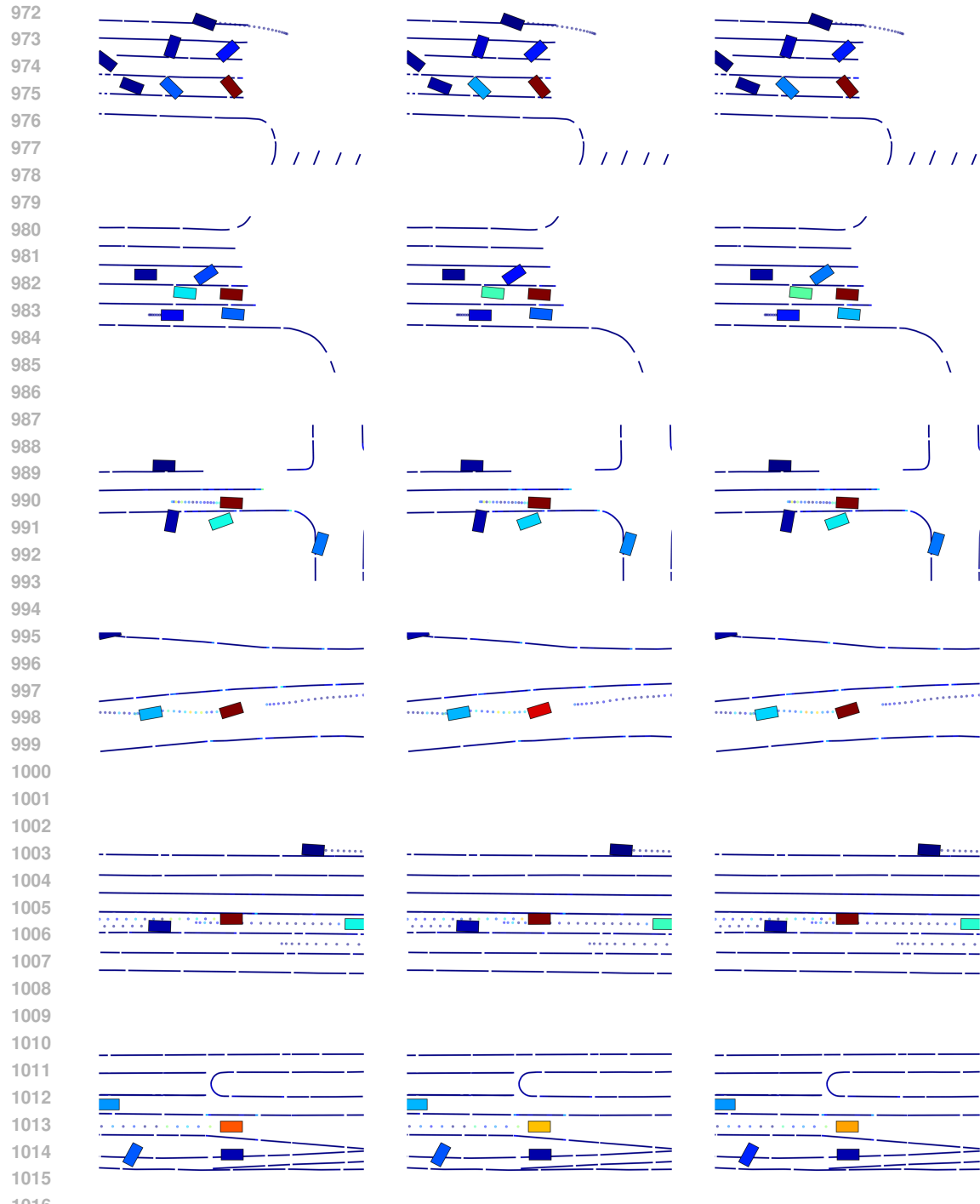
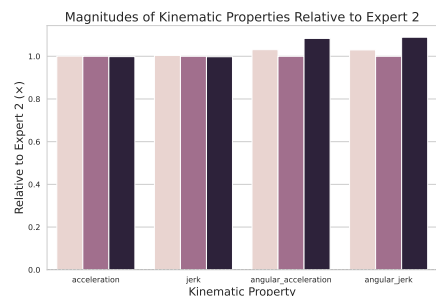
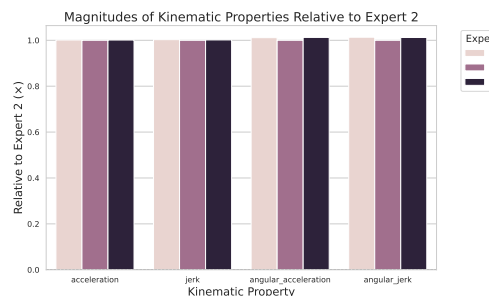


Figure 7: **Visualization of scenario feature saliency.** Saliency maps are visualized for 10 randomly selected scenarios from Argoverse on MTR+Actions (Left), Ours+CAT (Middle), and Ours+MoV (Right). The top 2 scenarios feature mostly stationary agents. In each scenario and model, the ego vehicle has the most saliency (colored red), followed by nearby agents and map polylines.

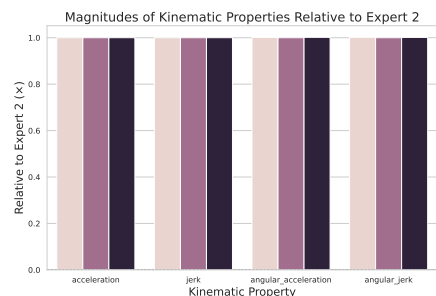
1026 H ADDITIONAL VISUALIZATIONS FOR RELATIVE KINEMATICS BY EXPERT



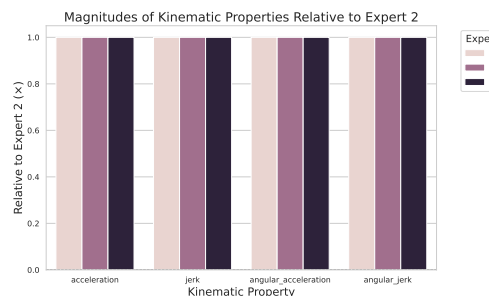
(a) C-Poly



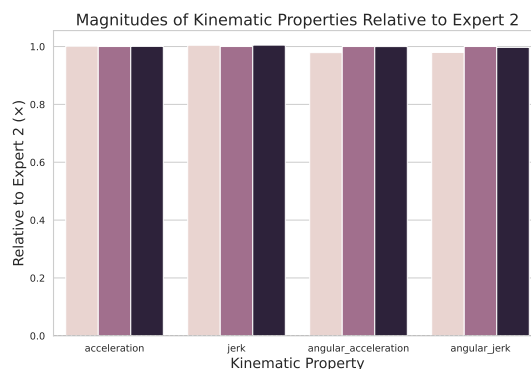
(b) HyperFormer



(c) Polytropion



(d) MoV



(e) CAT

Figure 8: **Kinematic magnitude comparisons for all variants of our approach.** Experiments run with seed 0 are plotted.

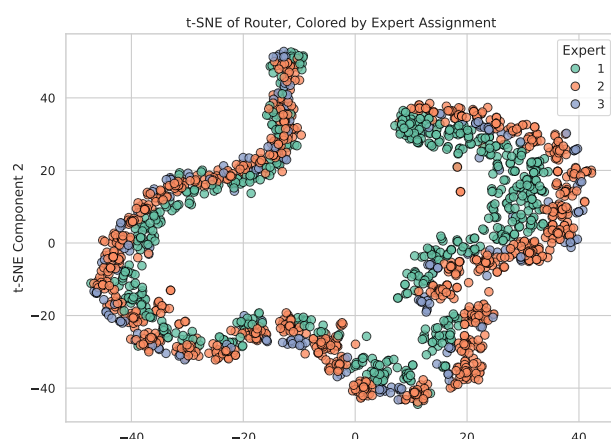
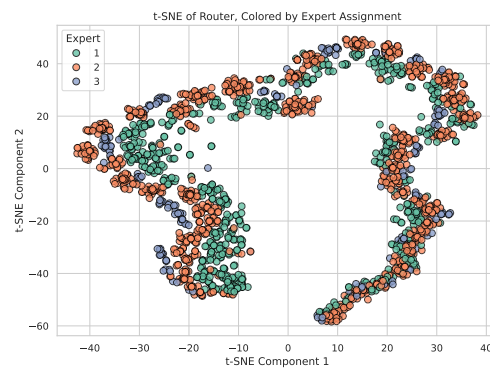
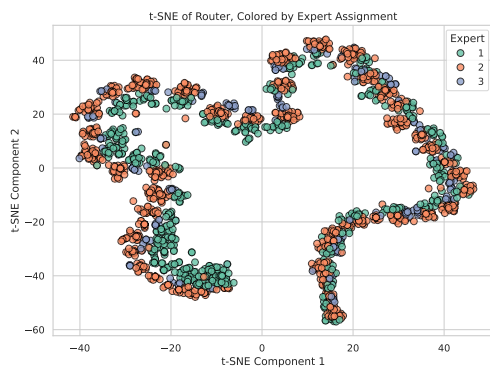
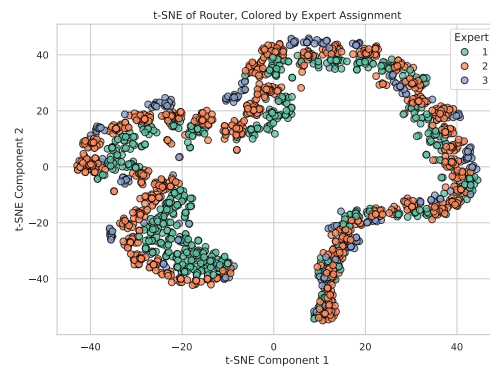
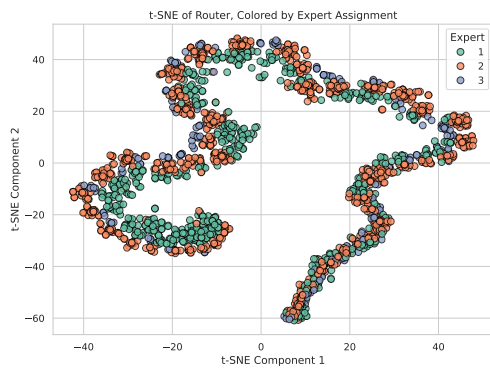
1080 I ADDITIONAL T-SNE PLOTS FOR ROUTER EMBEDDINGS BY EXPERT
1081
1082

Figure 9: **t-SNE visualization of router embeddings for all variants of our approach.** Experiments run with seed 0 are plotted.

1134 **J BASELINE MTR MODEL HYPERPARAMETERS**
1135
1136
11371138 Table 7: Hyperparameters used for training the MTR baseline model.
1139

Hyperparameter	Value
Context Encoder	
NAME	MTREncoder
NUM_OF_ATTN_NEIGHBORS	7
NUM_INPUT_ATTR_AGENT	39
NUM_INPUT_ATTR_MAP	29
NUM_CHANNEL_IN_MLP_AGENT	256
NUM_CHANNEL_IN_MLP_MAP	64
NUM_LAYER_IN_MLP_AGENT	3
NUM_LAYER_IN_MLP_MAP	5
NUM_LAYER_IN_PRE_MLP_MAP	3
D_MODEL	256
NUM_ATTN_LAYERS	6
NUM_ATTN_HEAD	8
DROPOUT_OF_ATTN	0.1
USE_LOCAL_ATTN	True
Motion Decoder	
NAME	MTRDecoder
NUM_MOTION_MODES	6
D_MODEL	512
NUM_DECODER_LAYERS	6
NUM_ATTN_HEAD	8
MAP_D_MODEL	256
DROPOUT_OF_ATTN	0.1
NUM_BASE_MAP_POLYLINES	256
NUM_WAYPOINT_MAP_POLYLINES	128
LOSS_WEIGHTS.cls	1.0
LOSS_WEIGHTS.reg	1.0
LOSS_WEIGHTS.vel	0.5
NMS_DIST_THRESH	2.5
Training	
max_epochs	40
learning_rate	0.0001
learning_rate_sched	[22, 24, 26, 28]
optimizer	AdamW
scheduler	lambdaLR
grad_clip_norm	1000.0
weight_decay	0.01
lr_decay	0.5
lr_clip	0.000001
WEIGHT_DECAY	0.01
train_batch_size	64
eval_batch_size	64
Data	
max_num_agents	64
map_range	100
max_num_roads	768
max_points_per_lane	20
manually_split_lane	True
point_sampled_interval	1
num_points_each_polyline	20
vector_break_dist_thresh	1.0
predict_actions	True

1188 **K POLYSONA MODEL HYPERPARAMETERS**
11891190
1191 Table 8: Hyperparameters used for training the PolySona models. Rows highlighted in yellow
1192 indicate differences from the baseline MTR configuration.

1193	1194	Hyperparameter	Value
1195	Context Encoder		
1196	NAME	MTREncoder	
1197	NUM_OF_ATTN_NEIGHBORS	7	
1198	NUM_INPUT_ATTR_AGENT	39	
1199	NUM_INPUT_ATTR_MAP	29	
1200	NUM_CHANNEL_IN_MLP_AGENT	256	
1201	NUM_CHANNEL_IN_MLP_MAP	64	
1202	NUM_LAYER_IN_MLP_AGENT	3	
1203	NUM_LAYER_IN_MLP_MAP	5	
1204	NUM_LAYER_IN_PRE_MLP_MAP	3	
1205	D_MODEL	256	
1206	NUM_ATTN_LAYERS	6	
1207	NUM_ATTN_HEAD	8	
1208	DROPOUT_OF_ATTN	0.1	
1209	USE_LOCAL_ATTN	True	
Motion Decoder			
1210	NAME	PolySonaDecoder	
1211	NUM_MOTION_MODES	6	
1212	INTENTION_POINTS_FILE	cluster_64_center_dict_6s.pkl	
1213	D_MODEL	512	
1214	NUM_DECODER_LAYERS	6	
1215	NUM_ATTN_HEAD	8	
1216	MAP_D_MODEL	256	
1217	DROPOUT_OF_ATTN	0.1	
1218	NUM_BASE_MAP_POLYLINES	256	
1219	NUM_WAYPOINT_MAP_POLYLINES	128	
1220	LOSS_WEIGHTS.cls	1.0	
1221	LOSS_WEIGHTS.reg	1.0	
1222	LOSS_WEIGHTS.vel	0.5	
1223	NMS_DIST_THRESH	1.0	
Training			
1224	max_epochs	10	
1225	learning_rate	0.001	
1226	learning_rate_sched	[22, 24, 26, 28]	
1227	optimizer	AdamW	
1228	scheduler	polynomialLR (power=2)	
1229	grad_clip_norm	1000.0	
1230	weight_decay	0.00	
1231	lr_decay	0.5	
1232	lr_clip	0.000001	
1233	train_batch_size	256	
1234	eval_batch_size	256	
1235	predict_actions	True	
1236	lora_rank	4	
1237	freeze_encoder	True	
1238	freeze_decoder	True	
1239	attention_only	False	
1240	num_personas	3	
1241	prior	[0.3, 0.6, 0.1]	
	λ_{recon}	50	
	λ_{KL}	50	
	λ_{entropy}	25	
	seed	0 / 1 / 2	
Data			
1242	max_num_agents	64	
1243	map_range	100	
1244	max_num_roads	768	
1245	max_points_per_lane	20	
1246	manually_split_lane	True	
1247	point_sampled_interval	1	
1248	num_points_each_polyline	20	
1249	vector_break_dist_thresh	1.0	

1242 L IMPACT OF RANK ON PERFORMANCE
12431244 Table 9: Comparison of Ours+CAT Across Different Ranks.
1245

Rank	brierFDE↓	minADE↓	minFDE↓	MissRate↓
2	2.1593	0.8573	1.7059	0.3151
4	2.1607	0.8624	1.7041	0.3171
8	2.1578	0.8578	1.7042	0.3120
16	2.1668	0.8610	1.7102	0.3151

1251
1252 Table 10: Comparison of Ours+CAT Across Different Ranks, Grouped by Kalman Difficulty
1253 and TDBM Driving Styles.
1254

Rank	Kalman Difficulty			TDBM Driving Styles			
	Easy	Medium	Hard	Timid	Careful	Reckless	Threatening
2	0.8120	1.1675	3.9875	0.8903	0.8865	0.8577	0.8172
4	0.8188	1.1678	2.4978	0.8793	0.8477	0.8655	0.8161
8	0.8130	1.1641	3.9882	0.8913	0.9833	0.8581	0.8183
16	0.8149	1.1758	4.2696	0.8944	0.8858	0.8613	0.8225

1261
1262
1263
1264
1265
1266
1267
1268
1269
1270
1271
1272
1273
1274
1275
1276
1277
1278
1279
1280
1281
1282
1283
1284
1285
1286
1287
1288
1289
1290
1291
1292
1293
1294
1295

1296 M STANDARD DEVIATION TABLE
12971298 Table 11: **Standard Deviation of Trajectory Prediction Benchmark Performance Comparisons.**
1299

1300 Method	1301	brierFDE \downarrow	minADE \downarrow	minFDE \downarrow	MissRate \downarrow
1302 Ours+Polytronon Ponti et al. (2023)	0.0004	0.0004	0.0004	0.0009	
1303 Ours+C-Poly Wang et al. (2024a)	0.0026	0.0011	0.0025	0.0003	
1304 Ours+HyperFormer Karimi Mahabadi et al. (2021)	0.0017	0.0004	0.0017	0.0010	
1305 Ours+CAT Prabhakar et al. (2024)	0.0019	0.0012	0.0018	0.0010	
Ours+MoV Zadouri et al. (2024)	0.0010	0.0007	0.0010	0.0004	

1306
1307 Table 12: **Standard Deviation of minADE Comparison by Kalman Difficulty and TDBM Driving
1308 Style groups.**
1309

1310 Method	1311 Kalman Difficulty			1312 TDBM Driving Styles			
	1313 Easy	1314 Medium	1315 Hard	1316 Timid	1317 Careful	1318 Reckless	1319 Threatening
Ours+PolyTropo Zadouri et al. (2024)	0.0003	0.0032	0.0040	0.0005	0.0038	0.0004	0.0005
Ours+C-Poly Wang et al. (2024a)	0.0013	0.0003	0.0146	0.0009	0.0286	0.0012	0.0011
Ours+HyperFormer Karimi Mahabadi et al. (2021)	0.0006	0.0013	0.0060	0.0006	0.0330	0.0004	0.0007
Ours+CAT Prabhakar et al. (2024)	0.0012	0.0051	0.0682	0.0014	0.0340	0.0012	0.0012
Ours+MoV Zadouri et al. (2024)	0.0007	0.0006	0.0041	0.0008	0.0026	0.0007	0.0006

Table 13: Hyperparameter sweep of # of classes used in PolySona training.

# Latent Classes	Easy / minADE	Medium / minADE	Hard / minADE	Overall minADE
2	0.8108	1.1951	3.5275	0.8589
3	0.8188	1.1678	2.4978	0.8624
4	0.8119	1.1990	3.5116	0.8603
5	0.8120	1.1996	3.5191	0.8605
6	0.8109	1.1986	3.5729	0.8595
8	0.8123	1.2027	3.4217	0.8610
10	0.8122	1.2007	3.6048	0.8609

N HYPERPARAMETER SWEET: NUMBER OF LATENT CLASSES MODELED

1350
1351
1352
1353
1354
1355
1356
1357
1358
1359
1360
1361
1362
1363
1364
1365
1366
1367
1368
1369
1370
1371
1372
1373
1374
1375
1376
1377
1378
1379
1380
1381
1382
1383
1384
1385
1386
1387
1388
1389
1390
1391
1392
1393
1394
1395
1396
1397
1398
1399
1400
1401
1402
1403